doi:10.1246/cl.130446

Unique Mesoporous Silicoaluminophosphate Assembled from Faujasite-type SAPO-37 Precursor: A Potential Catalyst for Isomerization

Rekha Yadav, Arvind Kumar Singh, and Ayyamperumal Sakthivel*
Department of Chemistry, Inorganic Materials and Catalysis Laboratory, University of Delhi, Delhi-110007, India

(Received May 13, 2013; CL-130446; E-mail: asakthivel@chemistry.du.ac.in)

Unique mesoporous silicoaluminophosphate (MESO-SAPO-37) with uniform pores (3 nm) was synthesized for the first time by using a faujasite-type microporous SAPO-37 precursor. MESO-SAPO-37 contains hierarchical mesopores with a microporous secondary building unit. It possesses strong acidity and shows high catalytic activity for the conversion of 1-octene, with the exclusive formation of isomerized products (84%).

Concern for natural resources and consideration of environmental impacts are essential for the development of better catalytic systems for various fine and petrochemical processes.[1,2] Zeolite and zeolite-like aluminophosphate materials are of great interest in this context, as they show good adsorptive and catalytic properties with flexible frameworks.[3] The limitations of these microporous molecular sieves have been overcome through the successful synthesis of mesoporous aluminosilicates such as the M41s family,[4] SBA-15,[5] HMS,[6] mesoporous titania,[7] and mesoporous aluminophosphate materials.[8] Several synthetic approaches such as hydrothermal and solvent-phase solvent-evaporation spray drying have been used for mesoporous materials.[9] These mesoporous molecular sieves have opened up new prospects and excellent opportunities in the area of heterogeneous catalysis, adsorption, and supports.[10–13] However, in general, their structures collapse at elevated temperatures because of their amorphous wall properties. The thermal and hydrothermal stabilities of mesoporous aluminosilicate were significantly improved through the synthesis of meso-micro-composites.[14,15] Many researchers have endeavored to develop meso-micro-aluminophosphate by generating mesoporosity on microporous silicoaluminophosphate (SAPO). Nevertheless, the resultant hierarchical microporous SAPO does not show any X-ray mesoporosity.[16] Attempts have also been made to convert the mesoporous silica into meso and micro silicoaluminophosphate materials, but their intrinsic properties have been similar to those of mesoporous silica.[17] The synthesis of meso and micro aluminophosphate-based materials is a great challenge and is still a subject of investigation. On the other hand, isomerized products of olefins are important feedstocks for various chemical processes, and SAPO-based molecular sieves have been shown as promising catalysts.[18] In particular, the microporous SAPO-37 faujasite-type molecular sieve is well known as a potential catalyst for various chemical transformations.[19] As far as we know, there have been no reports on the controlled synthesis of mesoporous silicoaluminophosphate from microporous structural secondary building units (SBUs) or on its applications.

In the present strategy, a microporous SAPO-37 precursor was used to assemble mesoporous silicoaluminophosphate (MESO-SAPO-37), as shown in Scheme 1. The cationic species resulting from cetyltrimethylammonium bromide (CTAB) interacts electrostatically with the preformed anionic SAPO-37 precursors. These interactions take place at interface between organic and inorganic phase in solution.[10d,10e] The resultant MESO-SAPO-37 possesses both microporous and mesoporous properties. MESO-SAPO-37 was shown to be a promising catalyst for the isomerization of 1-octene at ambient temperature in a liquid-phase medium, with the formation of only the isomerized product. The microporous SAPO-37 precursor was synthesized (Supporting Information, SI)[20] by using a modification of the literature procedure.[21] MESO-SAPO-37 was synthesized from the microporous precursor prepared with a crystallization time of 6 h in the presence of surfactant solution (SI).[20] The resultant materials were systematically characterized by various spectroscopic and analytical techniques (SI).[20]

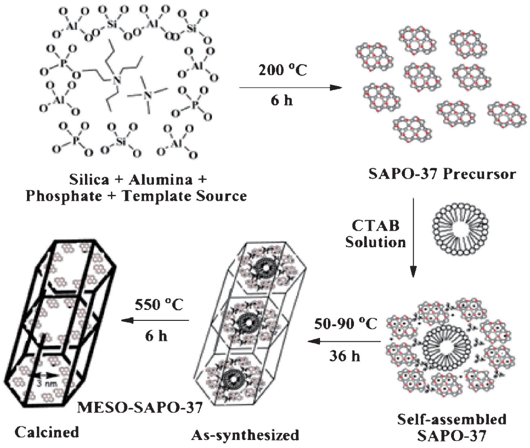

Scheme 1. Schematic representation of MESO-SAPO-37 synthesis.

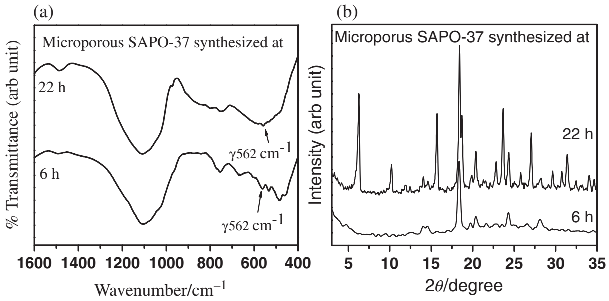

Figure 1. Nature of SAPO-37 precursors: (a) FTIR and (b) XRD data.

Fourier transform infrared (FTIR) spectra (Figure 1a) of the microporous precursors obtained at 6 and 22 h show a broad vibrational band in the region 530–565 cm^{-1}, which is characteristic of the structural secondary building unit of SAPO-37.[21,22] Complete crystalline SAPO-37 was obtained after 22 h. The

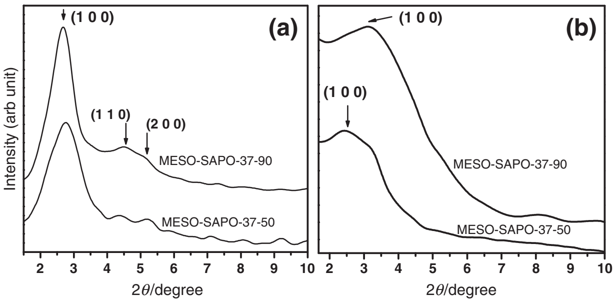

Figure 2. Powder X-ray diffraction patterns of MESO-SAPO-37: (a) as-synthesized and (b) calcined samples.

weak XRD reflection observed after 6 h of crystallization (Figure 1b) indicates that SAPO-37 structural secondary subunit formation started at this juncture. For the assembly of MESO-SAPO-37 having micro- and mesoporous properties, the SAPO-37 precursor obtained at 6 h was utilized.

MESO-SAPO-37 was synthesized (SI)[20] by using the SAPO-37 precursor in the presence of surfactant solution with a molar gel composition of $(TPA)_2O$:$(TMA)_2O$:Al_2O_3:P_2O_5:SiO_2:CTAB:H_2O = 1.0:2.1–2.8:1.0:1.0:0.43:0.45–0.60:226.94 (TPA: tetrapropylammonium, TMA: tetramethylammonium). The MESO-SAPO-37 materials prepared at 50 and 90 °C are represented as MESO-SAPO-37-50 and MESO-SAPO-37-90, respectively. The powder XRD patterns of the as-synthesized samples (Figure 2) show well-resolved peaks, which are indexed to the (100), (110), and (200) reflections of an ordered hexagonal structure.[4,8,11] The powder X-ray diffraction patterns of the calcined samples (Figure 2) exhibit a broad peak at 2.5–3.5°, indicating the presence of hierarchical mesostructures.[13] Further, the diffraction patterns in the higher 2θ region from 5 to 40° show weak reflections around 14, 18, and 24°, confirming the presence of microporous SAPO-37 units within the system (Figure S1, SI).[20] The FTIR spectra of MESO-SAPO-37 (Figure S2, SI)[20] retain the broad band in the region 530–565 cm^{-1} attributed to the SBU of SAPO-37, supporting the fact that MESO-SAPO-37 was assembled from the microporous precursor.

The nitrogen sorption isotherms of the MESO-SAPO-37 samples are shown in Figure 3. Both microporous and mesoporous features can be seen clearly in both samples. The samples showed type-IV isotherms (IUPAC)[23] with H4-type hysteresis for MESO-SAPO-37-90, corresponding to materials containing narrow slit-like pores,[23,24] and H2 and H3 types for MESO-SAPO-37-50, indicating the presence of bottleneck-type mesopores.[24] The sharp uptake in the isotherms at a relative pressure (p/p_0) of less than 0.01, associated with micropores,[23] arises from the structural SAPO-37 building unit. The textural properties of MESO-SAPO-37 are summarized in Table 1. In particular, MESO-SAPO-37-90 shows high surface areas (BET and DFT) and pore volumes (BJH, DFT, and HK) and uniform pore-size distributions (Figure S3, SI),[20] similarly to heteroatom-substituted mesoporous aluminophosphate materials.[13,23] It is noteworthy that MESO-SAPO-37 prepared above 90 °C resulted in the formation of the lamellar phase,[25] which collapsed upon calcination, leading to poor textural properties. The observed t-plot surface area and HK pore volume clearly confirmed the presence of a microporous structural subunit on the domain of MESO-SAPO-37. The relatively low overall surface area of MESO-SAPO-37 must be due to the presence of microporous SBUs on the walls of mesoporous channels.

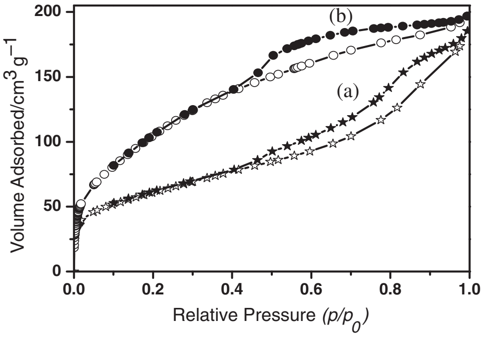

Figure 3. N_2 sorption isotherms of (a) MESO-SAPO-37-50 and (b) MESO-SAPO-37-90.

Table 1. Textural properties of MESO-SAPO-37

Samples[a]	Surface area /$m^2 g^{-1}$			Pore volume /$cm^3 g^{-1}$			BJH pore size /nm
	BET	DFT	t-plot	BJH	DFT	HK	
(a)	215	249	14	0.16	0.19	0.06	4.1
(b)	458	555	26	0.28	0.31	0.11	3.1

[a] (a) MESO-SAPO-37-50 and (b) MESO-SAPO-37-90.

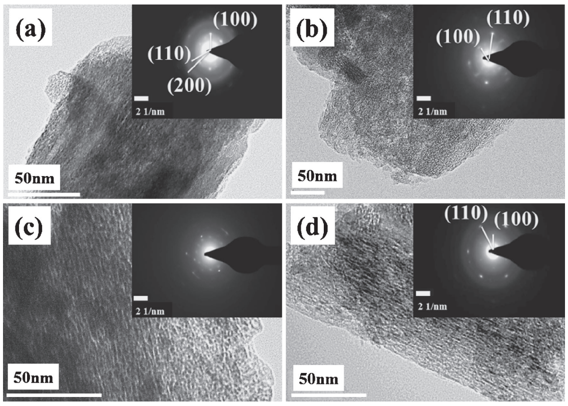

Figure 4. HRTEM images and ED patterns of as-synthesized (a) MESO-SAPO-37-50, (b) MESO-SAPO-37-90, and calcined (c) MESO-SAPO-37-50, and (d) MESO-SAPO-37-90.

Figure 4 shows the high-resolution transmission electron microscopy (HRTEM) images and electron diffraction (ED) patterns of the as-synthesized and calcined MESO-SAPO-37 samples. Both the as-synthesized and calcined MESO-SAPO-37 samples showed direct evidence for hierarchical mesopores, consistent with the XRD pattern. The regularly distributed pores in the range 3–4 nm with short-range order, which can be seen in the calcined samples, are in agreement with the surface-area analysis data. The ED pattern of calcined MESO-SAPO-37 further indicates that the walls of the mesopores are crystalline in nature.

The acidities of the microporous SAPO-37 and MESO-SAPO-37 were followed by pyridine-FTIR spectroscopy (Figure S4, SI);[20] the spectrum showed a broad vibrational band between 1440 and 1450 cm^{-1}, corresponding to pyridine bound

Table 2. Catalytic performance of MESO-SAPO-37[a]

Samples[b]	1-Octene Conv. /wt %	Selectivity				
		Linear octene			Iso-octene	Dimer product
		2-	3-	4-		
(a)	83.4	23.9	37.2	24.4	14.9	0
(b)	84.2	24.0	38.2	25.9	11.9	0
MESO-SAPO	16.6	41.7	40.3	18.0	0	0
SAPO-37	52.8	33.9	42.1	21.5	0	2.4
No catalyst	1.3	0	0	49.3[c]	0	0

[a]Reaction conditions: Temp, 200 °C; time, 6 h; catalyst, 200 mg; 1-octene, 20 mL. [b](a) MESO-SAPO-37-50 and (b) MESO-SAPO-37-90. [c]Remaining products are unidentified.

to proton-bonded, Lewis acidic sites, and a band around 1540 cm^{-1}, related to pyrdine bound to Brønsted acidic sites. An additional band around 1490 cm^{-1} is attributed to both pyridine-bound Lewis and Brønsted acidic sites.[11a] It is evident from the figure (Figure S4, SI)[20] that as the desorption temperature is increased from 200 to 500 °C, the intensity of the vibrational band corresponding to Brønsted acidic sites remains accountable, clearly indicating the presence of strong acidic sites in MESO-SAPO-37.

The catalytic performances of MESO-SAPO-37 and the conventional SAPO-37 were tested for the isomerization of 1-octene in a liquid-phase batch reactor (SI);[20] the results are given in Table 2. The major isomerization products in the case of MESO-SAPO-37 are 2-octene, 3-octene, 4-octene, and iso-octenes formed by the double-bond shift. In the absence of a catalyst, the reaction showed only about 1% conversion, which may be because of the presence of impurities in the reactant (1-octene, 98%). Microporous SAPO-37 showed around 53% 1-octene conversion with considerable amounts of dimerized products owing to the reaction occurring on the external surface. On the other hand, MESO-SAPO-37 showed a better 1-octene conversion of more than 84%, with selective formation of the isomerized products. The higher activity of the MESO-SAPO-37 catalyst is thought to be due to the presence of strong acidic sites and its hierarchical mesoporous nature with microporous domains, which favors the fast diffusion of reactant molecules.

In summary, the mesoporous silicoaluminophosphate system having microporous faujasite-type SAPO-37 building units has been synthesized for the first time. The resultant MESO-SAPO-37 possesses mesoporous channels with microporous wall properties. MESO-SAPO-37 shows exclusively isomerized products on the conversion of 1-octene under ambient conditions in the liquid-phase medium.

DST and University of Delhi, India are acknowledged for their support. RY, AKS also thanks UGC & CSIR for their JRF.

References and Notes

1 a) F. Zaera, *Chem. Soc. Rev.* **2013**, *42*, 2746. b) M. J. Climent, A. Corma, S. Iborra, *Chem. Rev.* **2011**, *111*, 1072. c) W. Vermeiren, J.-P. Gilson, *Top. Catal.* **2009**, *52*, 1131. d) J. Čejka, S. Mintova, *Catal. Rev.* **2007**, *49*, 457.

2 a) S. G. Anagho, H. M. Ngomo, in *Petrochemicals: Cellulosic Wastes as an Alternative Source of Feedstock*, ed. by V. Patel, InTech, **2012**, Chap. 1. doi:10.5772/37782. b) J. Nishino, M. Itoh, T. Ishinomori, N. Kubota, Y. Uemichi, *J. Mater. Cycles Waste Manage.* **2003**, *5*, 89.

3 a) J. Li, J. Yu, R. Xu, *Proc. R. Soc. A* **2012**, *468*, 1955. b) E. M. Flanigen, R. W. Broach, S. T. Wilson, in *Zeolites in Industrial Separation and Catalysis*, ed. by S. Kulprathipanja, Weinheim, Wiley-VCH, **2010**, Chap. 1, p. 1. doi:10.1002/9783527629565.ch1. c) B. Yilmaz, U. Müller, *Top. Catal.* **2009**, *52*, 888. d) J. Yu, R. Xu, *Chem. Soc. Rev.* **2006**, *35*, 593. e) H. O. Pastore, S. Coluccia, L. Marchese, *Annu. Rev. Mater. Res.* **2005**, *35*, 351. f) J. M. Thomas, R. Raja, G. Sankar, R. G. Bell, *Acc. Chem. Res.* **2001**, *34*, 191.

4 C. T. Kresge, M. E. Leonowicz, W. J. Roth, J. C. Vartuli, J. S. Beck, *Nature* **1992**, *359*, 710.

5 a) D. Zhao, J. Feng, Q. Huo, N. Melosh, G. H. Fredrickson, B. F. Chmelka, G. D. Stucky, *Science* **1998**, *279*, 548. b) Q. Huo, D. I. Margolese, U. Ciesla, P. Feng, T. E. Gier, P. Sieger, R. Leon, P. M. Petroff, F. Schüth, G. D. Stucky, *Nature* **1994**, *368*, 317.

6 P. T. Tanev, T. J. Pinnavaia, *Science* **1995**, *267*, 865.

7 a) Y. Yamauchi, N. Suzuki, L. Radhakrishnan, L. Wang, *Chem. Rec.* **2009**, *9*, 321. b) K. Ariga, A. Vinu, Y. Yamauchi, Q. Ji, J. P. Hill, *Bull. Chem. Soc. Jpn.* **2012**, *85*, 1. c) J. L. Vivero-Escoto, Y.-D. Chiang, K. C.-W. Wu, Y. Yamauchi, *Sci. Technol. Adv. Mater.* **2012**, *13*, 013003.

8 a) S. Oliver, A. Kuperman, N. Coombs, A. Lough, G. A. Ozin, *Nature* **1995**, *378*, 47. b) A. Sayari, V. R. Karra, J. S. Reddy, I. L. Moudrakovski, *Chem. Commun.* **1996**, 411. c) B. Chakraborty, A. C. Pulikottil, S. Das, B. Viswanathan, *Chem. Commun.* **1997**, 911. d) D. Zhao, Z. Luan, L. Kevan, *Chem. Commun.* **1997**, 1009. e) J. O. Perez, R. B. Borade, A. Clearfield, *J. Mol. Struct.* **1998**, *470*, 221.

9 a) T. Kimura, K. Kato, Y. Yamauchi, *Chem. Commun.* **2009**, 4938. b) T. Kimura, Y. Yamauchi, *Langmuir* **2012**, *28*, 12901.

10 a) C. Perego, R. Millini, *Chem. Soc. Rev.* **2013**, *42*, 3956. b) Z. Wu, D. Zhao, *Chem. Commun.* **2011**, *47*, 3332. c) K. Ariga, Q. Ji, J. P. Hill, A. Vinu, *Soft Mater.* **2009**, *5*, 3562. d) B. Xu, C. Zhao, Z. Yan, *J. Nat. Gas Chem.* **2005**, *14*, 65. e) Z. A. ALOthman, *Materials* **2012**, *5*, 2874.

11 a) A. Sakthivel, S. E. Dapurkar, N. M. Gupta, S. K. Kulshreshtha, P. Selvam, *Microporous Mesoporous Mater.* **2003**, *65*, 177. b) A. Sakthivel, J. Zhao, F. E. Kühn, *Microporous Mesoporous Mater.* **2005**, *86*, 341.

12 a) P. Selvam, A. Sakthivel, in *Liquid Phase Oxidation via Heterogeneous Catalysis: Organic Synthesis and Industrial Applications*, ed. by M. G. Clerici, O. A. Kholdeeva, Wiley Interscience, **2013**, pp. 95–125, and reference therein. doi:10.1002/9781118356760.ch3. b) Y. Shi, Y. Wan, D. Zhao, *Chem. Soc. Rev.* **2011**, *40*, 3854. c) T. Kimura, *Microporous Mesoporous Mater.* **2005**, *77*, 97, and references are cited therein.

13 a) P. Zhang, L. Wang, L. Ren, L. Zhu, Q. Sun, J. Zhang, X. Meng, F.-S. Xiao, *J. Mater. Chem.* **2011**, *21*, 12026. b) T. D. Conesa, R. Mokaya, Z. Yang, R. Luque, J. M. Campelo, A. A. Romero, *J. Catal.* **2007**, *252*, 1. c) L. Wang, B. Tian, J. Fan, X. Liu, H. Yang, C. Yu, B. Tu, D. Zhao, *Microporous Mesoporous Mater.* **2004**, *67*, 123.

14 a) I. I. Ivanova, E. E. Knyazeva, *Chem. Soc. Rev.* **2013**, *42*, 3671. b) K. Möller, T. Bein, *Chem. Soc. Rev.* **2013**, *42*, 3689. c) L.-H. Chen, X.-Y. Li, J. C. Rooke, Y.-H. Zhang, X.-Y. Yang, Y. Tang, F.-S. Xiao, B.-L. Su, *J. Mater. Chem.* **2012**, *22*, 17381. d) Z. L. Hua, J. Zhou, J. L. Shi, *Chem. Commun.* **2011**, *47*, 10536.

15 a) A. Sakthivel, K. Komura, S.-J. Huang, P.-H. Wu, S.-B. Liu, Y. Sasaki, Y. Sugi, *Ind. Eng. Chem. Res.* **2010**, *49*, 65. b) A. Sakthivel, S.-J. Huang, W.-H. Chen, Z.-H. Lan, K.-H. Chen, H.-P. Lin, C.-Y. Mou, S.-B. Liu, *Adv. Funct. Mater.* **2005**, *15*, 253. c) D. T. On, S. Kaliaguine, *Angew. Chem., Int. Ed.* **2002**, *41*, 1036. d) Y. Liu, T. J. Pinnavaia, *J. Mater. Chem.* **2002**, *12*, 3179. e) Z. Zhang, Y. Han, L. Zhu, R. Wang, Y. Yu, S. Qiu, D. Zhao, F.-S. Xiao, *Angew. Chem., Int. Ed.* **2001**, *40*, 1258.

16 a) S.-T. Yang, J.-Y. Kim, H.-J. Chae, M. Kim, S.-Y. Jeong, W.-S. Ahn, *Mater. Res. Bull.* **2012**, *47*, 3888. b) J. Liang, F. P. Wang, *Adv. Mater. Res.* **2011**, *306–307*, 1576. c) H. Yang, Z. Liu, H. Gao, Z. Xie, *J. Mater. Chem.* **2010**, *20*, 3227. d) N. Danilina, F. Krumeich, J. A. van Bokhoven, *J. Catal.* **2010**, *272*, 37.

17 a) Y. Liu, L. Wang, J. Zhang, L. Chen, H. Xu, *Microporous Mesoporous Mater.* **2011**, *145*, 150. b) T. D. Conesa, R. Mokaya, J. M. Campelo, A. A. Romero, *Chem. Commun.* **2006**, 1839.

18 a) Y. Fan, H. Xiao, G. Shi, H. Liu, X. Bao, *J. Catal.* **2012**, *285*, 251. b) C. M. López, L. Ramírez, V. Sazo, V. Escobar, *Appl. Catal., A* **2008**, *340*, 1.

19 I. Fechete, Y. Wang, J. C. Védrine, *Catal. Today* **2012**, *189*, 2.

20 Experimental section, high-angle powder XRD, FTIR, PSD of MESO-SAPO-37, and Pyridine FTIR spectra (Figures S1–S4). Supporting Information is available electronically on the CSJ-Journal Web site, http://www.csj.jp/journals/chem-lett/index.html.

21 L. S. de Saldarriaga, C. Saldarriaga, M. E. Davis, *J. Am. Chem. Soc.* **1987**, *109*, 2686.

22 A. F. Ojo, J. Dwyer, J. Dewing, K. Karim, *J. Chem. Soc., Faraday Trans.* **1991**, *87*, 2679.

23 a) M. Kruk, M. Jaroniec, *Chem. Mater.* **2001**, *13*, 3169. b) K. S. W. Sing, D. H. Everett, R. A. W. Haul, L. Moscou, R. A. Pierotti, J. Rouquérol, T. Siemieniewska, *Pure Appl. Chem.* **1985**, *57*, 603.

24 a) T. Mathew, K. Sivaranjani, E. S. Gnanakumar, Y. Yamada, T. Kobayashi, C. S. Gopinath, *J. Mater. Chem.* **2012**, *22*, 13484. b) K. Sivaranjani, C. S. Gopinath, *J. Mater. Chem.* **2011**, *21*, 2639.

25 Q. Huo, D. I. Margolese, G. D. Stucky, *Chem. Mater.* **1996**, *8*, 1147.